

Identification of a Two EF-Hand Ca^{2+} Binding Domain in Lobster Skeletal Muscle Ryanodine Receptor/ Ca^{2+} Release Channel^{†,‡}

Hui Xiong,^{§,⊥} Xiaoyong Feng,[⊥] Ling Gao, Le Xu, Daniel A. Pasek, Jeong-Ho Seok,^{||} and Gerhard Meissner*

Department of Biochemistry and Biophysics, University of North Carolina, Chapel Hill, North Carolina 27599-7260

Received May 21, 1997; Revised Manuscript Received February 10, 1998

ABSTRACT: The lobster skeletal muscle Ca^{2+} release channel, known also as the ryanodine receptor, is composed of four polypeptides of ~5000 amino acids each, like its mammalian counterparts. Clones encoding the carboxy-terminal region of the lobster ryanodine receptor were isolated from a lobster skeletal muscle cDNA library. Analysis of the deduced 1513 carboxy-terminal amino acid sequence suggests a cytoplasmic Ca^{2+} binding domain consisting of two EF-hand Ca^{2+} binding motifs (amino acid residues 594–656). The Ca^{2+} binding properties of this domain were assessed by preparing bacterial fusion proteins with sequences from the lobster Ca^{2+} binding domain and the corresponding sequences of the rabbit cardiac and skeletal muscle ryanodine receptors. The lobster skeletal muscle fusion protein bound $^{45}\text{Ca}^{2+}$ in Ca^{2+} overlays, and bound two Ca^{2+} under equilibrium binding conditions with a Hill dissociation constant (K_H) of 0.9 mM and coefficient (n_H) of 1.4. Rabbit skeletal and cardiac fusion proteins bound two Ca^{2+} with K_{HS} of 3.7 and 3.8 mM and n_{HS} of 1.1 and 1.3, respectively. Similar to results previously reported for the mammalian RyRs, the lobster RyR was activated by micromolar Ca^{2+} and inhibited by millimolar Ca^{2+} , as determined in single-channel and [^3H]ryanodine binding measurements. These results suggest that the two EF-hand Ca^{2+} binding domain of the lobster Ca^{2+} release channel as well as the corresponding regions of the mammalian channels may play a role in Ca^{2+} inactivation of sarcoplasmic reticulum Ca^{2+} release.

Ryanodine receptors (RyRs)¹ constitute a family of Ca^{2+} release channels that have an important role in Ca^{2+} signaling in muscle and nonmuscle cells by releasing Ca^{2+} from intracellular stores. One feature shared by all members of the RyR/ Ca^{2+} release channel family is their regulation by Ca^{2+} . Typically, RyRs are activated by micromolar cytoplasmic Ca^{2+} and inhibited by millimolar Ca^{2+} (1, 2). This biphasic behavior may result from at least two classes of Ca^{2+} binding sites, a high-affinity activation site and a low-affinity inactivation site. However, the location of these sites has not been established. Identification of Ca^{2+} binding sites has been hindered by the absence of clearly identifiable Ca^{2+} binding motifs in the primary deduced amino acid sequence of the RyR family which includes three mammalian (skeletal,

RyR1, refs 3, 4; cardiac, RyR2, refs 5, 6; brain, RyR3, ref 7), two amphibian (α and β corresponding to RyR1 and RyR3, ref 8), one avian (RyR3, ref 9), and one *Drosophila* (10) homologue.

Indirect evidence for the presence of several Ca^{2+} -sensitive RyR domains has been obtained for the mammalian skeletal muscle RyR. Several point mutations in the N-terminal and central regions of the human skeletal muscle RyR link to a rare muscle disorder known as malignant hyperthermia, which is characterized by elevated Ca^{2+} release from the sarcoplasmic reticulum (SR) (11). Several regions of the mammalian RyRs (3, 5, 7) bear some resemblance to the EF-hand Ca^{2+} binding motif of Ca^{2+} binding proteins. First characterized in the crystal structure of parvalbumin (12), the EF-hand Ca^{2+} binding motif has been found in other families of Ca^{2+} binding proteins including calmodulin, troponin C, and calbindin (13). The motif consists of a 12-amino acid residue loop flanked by two α -helices. Two or three helix-loop-helix structures can be present in a Ca^{2+} binding domain.

In the present study, we partially cloned and sequenced the cDNA encoding the lobster skeletal muscle Ca^{2+} release channel. As in cardiac muscle, in crustacean skeletal muscle the SR Ca^{2+} release channel is opened by Ca^{2+} ions that enter cells during a muscle action potential in a process known as Ca^{2+} -induced Ca^{2+} release (14, 15). A Ca^{2+} binding domain comprised of two EF-hand Ca^{2+} binding motifs was identified. The Ca^{2+} binding properties of this domain were determined in $^{45}\text{Ca}^{2+}$ overlays and by equilibrium binding dialysis using lobster skeletal muscle, rabbit

[†] Support by National Institutes of Health Grants AR18687 and HL27430 is gratefully acknowledged.

[‡] The nucleotide sequence in this paper has been submitted to GenBank with accession number AF051936.

* Author to whom correspondence should be addressed at Department of Biochemistry and Biophysics, University of North Carolina, Chapel Hill, NC 27599-7260. Tel: (919) 966-5021. Fax: (919) 966-2852. E-mail: gmeissne.biochem@mhs.unc.edu.

[§] Present address: Cleveland Clinic Florida, 3000 W. Cypress Creek Rd., Fort Lauderdale, FL 33309.

[⊥] Present address: Department of Pharmacology, College of Medicine, Chungnam National University, Taejeon 301-131, South Korea.

^{||} H. Xiong and X. Feng contributed equally to this work.

¹ Abbreviations: RyR, ryanodine receptor; SR, sarcoplasmic reticulum; EGTA, ethylene glycol-bis(β -aminoethyl ether)-*N,N,N',N'*-tetraacetic acid; BAPTA, 1,2-bis(2-aminophenoxy)ethanetetraacetic acid; LEF, lobster RyR EF-hand; CEF, region of rabbit cardiac muscle RyR corresponding to LEF; REF, region of rabbit skeletal muscle RyR corresponding to LEF.

skeletal muscle, and rabbit cardiac muscle fusion proteins. Our data indicate that the lobster Ca²⁺ binding domain and, by extension the less-well-conserved corresponding domains of the mammalian RyRs, may play a role in Ca²⁺ inactivation of channel activity.

EXPERIMENTAL PROCEDURES

Materials. [³H]Ryanodine was obtained from DuPont NEN, and unlabeled ryanodine was from AgriSystems International (Wind Gap, PA). Pefabloc SC (a protease inhibitor) was purchased from Boehringer Mannheim, and phospholipids were from Avanti (Birmingham, AL). All other chemicals were of analytical grade.

cDNA Cloning and Sequence Analysis. A cDNA library was prepared and screened using standard procedures. Poly (A)⁺ RNA was purified from total RNA (16) of lobster abdominal muscle using oligo dT-cellulose spin columns (Pharmacia Biotech, Piscataway, NJ). A size-selected (>1kb) lobster cDNA library was constructed in phage expression vector λ ZAP II by priming with random and oligo dT primers (Stratagene, La Jolla, CA). The cDNA library was screened using an affinity purified polyclonal antibody raised against the purified lobster RyR (17) according to a protocol provided by Stratagene. Phage from individual positive plaques were excised in the presence of helper phage R408 to form inserts containing plasmid Bluescript. Sequenase II and TAQuence II Kits (U.S. Biochemical, Cleveland, OH) were used to perform denatured, double-stranded DNA sequencing using M-13 and sequence-specific oligonucleotide primers. The DNA sequences and peptide sequences were assembled and analyzed using the University of Wisconsin Genetics Computer Group program package.

Expression of Lobster Ca²⁺ Binding Domain and Corresponding Rabbit Skeletal and Cardiac Muscle Domains in *Escherichia coli*. cDNA encoding the lobster RyR putative Ca²⁺ binding domain (Arg590 to Ile660, corresponding to positions 603–673 in Figure 1A) containing the two EF-hand motifs (LEF) was amplified by PCR. The product was cloned into *Bam*HI site of pET11d expression vector (Novagen, Madison, WI) to express pET-LEF, or into *Bam*HI and *Eco*RI sites of pGEX-3X expression vector (Pharmacia Biotech) to express GST-LEF. cDNAs coding for the corresponding regions of the rabbit skeletal RyR (Lys4069 to Ile4139, ref 3) and cardiac RyR (Lys4025 to Ile4095, ref 6) were obtained by PCR amplification of rabbit skeletal muscle and rabbit cardiac muscle (Stratagene) cDNA library, respectively, and were cloned into pET11d and pGEX-3X in the same fashion to express the corresponding regions of the rabbit skeletal (REF) and rabbit cardiac (CEF) muscle RyRs. The sequences of all constructs were confirmed by direct sequencing. pET-fusion peptides were analyzed, without purification, by SDS-PAGE, immunoblot, and ⁴⁵Ca²⁺ overlay. GST-fusion proteins were expressed as soluble proteins and purified to an extent of greater than 95% following a manual provided by Pharmacia Biotech for the GST expression system, before being used for measurement of ⁴⁵Ca²⁺ binding by equilibrium binding dialysis.

⁴⁵Ca²⁺ Overlays. Ca²⁺ binding studies were carried out using the overlay method described by Maruyama et al. (18). Proteins of bacterial lysates were denatured and separated in 12% tricine-SDS-polyacrylamide gels (19). After

transfer to nitrocellulose membranes at 300 mA for 1 h, the blots were washed with buffer A (60 mM KCl, 10 mM imidazole, pH 6.8) containing 5 mM MgCl₂ for 1 h with two changes. After two 5 min washes with buffer A, blots were incubated in buffer A containing 3 μ M ⁴⁵Ca²⁺ (2 μ Ci/mL) for 10 min at room temperature. The blots were then washed twice for 5 min in 50% ethanol, air-dried, exposed to X-ray film (Kodak, X-MAT), and quantified by densitometry.

Measurement of ⁴⁵Ca²⁺ Binding by Equilibrium Dialysis. ⁴⁵Ca²⁺ binding properties of GST-fusion proteins were determined by equilibrium dialysis using two 250 μ L chambers separated by a dialysis membrane with a molecular mass cutoff of 12000–14000 daltons. Purified GST-fusion proteins (~1 mg in 200 μ L) in binding buffer B (150 mM KCl, 10 mM imidazole, pH 7.0) were loaded into the left-chamber. The same amount of binding buffer B containing different Ca²⁺ concentrations (10 μ M to 10 mM) as well as trace amounts of ⁴⁵Ca²⁺ (0.5 μ Ci/mL) was loaded into the right chamber. Both the dialysis membrane and the two chambers were extensively washed with ddH₂O before use. Typically, 12–14 loaded chambers were gently rotated on a machine at room temperature for 24 h. Three aliquots of 50 μ L or two aliquots of 75 μ L binding buffer were taken from each chamber and their radioactivity was determined by liquid scintillation counting. Ca²⁺ binding to fusion proteins was determined as the difference in ⁴⁵Ca²⁺ content of left and right chambers.

Isolation of Sarcoplasmic Reticulum Vesicles and 30S Ca²⁺ Release Channel Complexes. Heavy SR vesicles were prepared from lobster abdominal muscle, rabbit skeletal muscle, and canine cardiac muscle, and the CHAPS-solubilized lobster 30S RyR complex was isolated as described (17). The purified lobster RyR was reconstituted into proteoliposomes by dialysis for 44 h at 4 °C against a 500 mM NaCl, 10 mM NaHepes, pH 7.4 buffer containing 0.1 mM EGTA, 0.2 mM CaCl₂, 0.2 mM PMSF, and 0.5 mM DTT (20). Proteoliposomes were sedimented by centrifugation (200000g for 2 h), resuspended in 250 mM NaCl, 10 mM NaPipes, pH 7.4, and stored at –135 °C.

Single-Channel Recordings. Single-channel measurements were performed at 23–25 °C by fusing proteoliposomes containing the purified lobster skeletal muscle RyR or lobster SR vesicles with Mueller–Rudin type bilayers containing phosphatidylethanolamine, phosphatidylserine, and phosphatidylcholine in the ratio 5:3:2 (25 mg of total phospholipid per mL of (*n*-decane) (21). The side of the bilayer to which the channels were added was defined as the cis side. The trans side of the bilayer was defined as ground. Single purified lobster channels were fused with bilayers using an asymmetric KCl, 20 mM KPipes, pH 7.0 buffer [50 mM trans (SR lumenal) KCl/250 mM cis (cytosolic) KCl] and recorded after increasing KCl concentration in the trans chamber to 250 mM. Lobster SR vesicles were fused using 50 mM trans CaHepes, pH 7.3/800 mM cis cholineCl, 0.5 mM CaCl₂, and recorded after perfusion of the cis chamber with 125mM TrisHepes, pH 7.3. Buffer solutions contained the additions indicated in the text. A strong dependence of single-channel activities on cis Ca²⁺ concentration (see Results) indicated that the large cytosolic “foot” region of the channel faced the cis chamber in a majority (> 98%) of

[illegible]

		EF1					EF2				
		X Y Z -X -Z					X Y Z -X -Z				
RyR1}	KLKD	IVGSEAFQDY	<u>VTDP</u>	<u>RG</u>	<u>LISK</u>	KDFQKAMDSQ	KQFTGPEIQF	LLSCSEADEN	EMINFEFFAN	RFQEPARDIG	
RyR2}	KLKD	LTSSDTFKEY	<u>DPDG</u>	<u>KGI</u>	<u>ISK</u>	RDFHKAMESH	KHYTQSETEF	LLSCAETDEN	ETLDYEEFVK	RFHEPAKDIG	
RyR3}	KLKD	LTSSDTFKEY	<u>DPDG</u>	<u>KGI</u>	<u>ISK</u>	KEFQKAMEGQ	KQYTQSEIDE	LLSCAETDEN	DMFNIDFVD	RFHEPAKDIG	
D}	KLAD	LIESPSFHEV	<u>DMK</u>	<u>NEG</u>	<u>WVTP</u>	KDFREKMEQS	KNYTPEEMDF	LLACCERNHE	GKIDYRAFE	HFHEPSKEIG	
Lob}	KLKD	LTSSDTFQEL	<u>DMNK</u>	<u>DGT</u>	<u>VTP</u>	AEFKEKMEQQ	KNYTTEINF	LLMCCDCNHD	GKIDYVEFTE	RFHNPKEIG	

FIGURE 1: Partial deduced amino acid sequence of lobster skeletal muscle RyR and putative Ca²⁺ binding domain. (A) Partial deduced amino acid sequences of rabbit skeletal muscle RyR (RyR1, ref 3), rabbit cardiac muscle RyR (RyR2, ref 6), lobster skeletal muscle RyR (Lob), and consensus sequence (Con). The two EF-hand Ca²⁺ binding motif of lobster RyR is shown in bold letters, and the putative transmembrane segments M1–M4 are underlined. Position 1 of skeletal and cardiac muscle RyR sequences corresponds to positions 3491 and 3448 of amino acid sequences published by Takeshima et al. (3) and Otsu et al. (6), respectively. (B) Alignment of the EF-hand structure of lobster RyR (Lob) to similar regions of rabbit skeletal muscle (RyR1) (3), rabbit cardiac muscle (RyR2) (6), rabbit brain (RyR3) (7), and *Drosophila* (D) (10) sequences. The positions of the oxygen-containing residues that are thought to be required for Ca²⁺ binding (X, Y, Z, -X, -Z) as defined by Kretsinger and Nockolds (12) are indicated. Mismatched residues in the Ca²⁺ binding regions are underlined.

recordings. Electrical signals were filtered at 2 kHz, digitized at 10 kHz, and analyzed as described (21).

[³H]Ryanodine Binding. Vesicles (250 µg protein/mL) were incubated with 2 nM [³H]ryanodine in media containing 125 mM KCl, 20 mM imidazole, pH 7.0, 0.2 mM Pefabloc SC, 20 µM leupeptin, and the indicated concentrations of Ca²⁺. Nonspecific binding was determined using a 1000-fold excess of unlabeled ryanodine. After 24–36 h at 24 °C, aliquots were diluted with 20 volumes of ice-cold water and placed on Whatman GF/B filters preincubated with 2% polyethyleneimine in water. Filters were washed with 3 × 5 mL of ice-cold 0.1 M KCl, 1 mM KPipes, pH 7.0 medium. The radioactivity remaining with the filters was determined by liquid scintillation counting to obtain bound [³H]ryanodine.

Other Biochemical Assays. Protein concentrations were determined with BCA protein assay reagent (Sigma, St Louis, MO) using bovine serum albumin as a standard. Free Ca²⁺ concentrations of > 1 µM were determined at 24 °C with a Ca²⁺-selective electrode (World Precision Instruments, Inc., Sarasota, FL) using Ca²⁺ standards obtained from Molecular Probes (Eugene, OR). Free Ca²⁺ concentrations of < 1 µM were obtained using stability constants and a computer program published by Shoenmakers et al. (22).

RESULTS

Cloning of Lobster Skeletal Muscle RyR. A lobster skeletal muscle cDNA library was constructed in phage expression vector λZAP II using mRNA isolated from lobster abdominal muscle. The library was screened with an affinity-purified polyclonal antibody against the purified full-length lobster RyR (17). Twelve positive plaques were obtained. To exclude false positive clones, degenerate PCR primers based on the most conserved carboxy-terminal region of the known RyR cDNA sequences were prepared. Four overlapping clones were isolated and sequenced. These clones code for 1513 carboxy-terminal residues of the approximately 5000 amino acids of the homologous mammalian RyRs (Figure 1A).

The deduced peptide sequence has 82% sequence similarity with the *Drosophila* RyR and 71–72% with mammalian RyR1, RyR2, and RyR3, amphibian RyR1 and RyR3 and avian RyR3. Hydrophathy analysis shows four hydrophobic segments at the C-terminal region which are highly conserved in all RyRs studied (Figure 1A, underlined), suggesting the presence of at least four transmembrane segments as first proposed by Takeshima et al. (3). The highly conserved

transmembrane region is consistent with the observation that the channel conducting properties of lobster RyR are close to those of mammalian RyRs (17). Analysis of potential ligand binding sites indicates the presence of two EF-hand Ca²⁺ binding motifs (amino acids 594–656, corresponding to positions 607–669 in Figure 1A, bold letters) which are partially conserved in *Drosophila* and the mammalian counterparts (Figure 1B). This potential Ca²⁺ binding domain is cytoplasmic in the membrane topology model of Takeshima et al. (3). A nucleotide binding consensus sequence GXGXXG (384–389, corresponding to positions 391–397 in Figure 1A) is conserved in *Drosophila*, but not in mammalian sequences.

⁴⁵Ca²⁺ Overlays of pET-Fusion Proteins. Ca²⁺ binding to the putative Ca²⁺ binding domain of the lobster skeletal muscle RyR and the corresponding regions of the rabbit skeletal and cardiac muscle RyRs was determined in ⁴⁵Ca²⁺ overlays, using fusion proteins expressed in *E. coli* with a 12 amino acid residue amino-terminal Tag sequence. Figure 2A shows a Coomassie Blue-stained gel of whole cell lysates from cells expressing pET11d alone (Ctl), the lobster skeletal muscle (LEF), rabbit skeletal muscle (REF), and rabbit cardiac muscle (CEF) pET-fusion peptides. The three fusion peptides were identified by immunoblot using a T7-Tag monoclonal antibody (Novagen) (Figure 2B). The rabbit skeletal peptide showed a lower staining reaction, even though amounts comparable to those of LEF appeared to be expressed (bottom band of lanes 2 and 3 of Figure 2A). LEF bound ⁴⁵Ca²⁺ at a position indicated by the antibody (Figure 2C), whereas only close to background binding was detected in the control (Ctl), REF, and CEF lanes. ⁴⁵Ca²⁺ binding to LEF decreased by 29% and 37% in the presence of 1 and 5 mM Mg²⁺, respectively, and by 71% in the presence of 10 µM ruthenium red in an overlay buffer containing 3 µM free Ca²⁺ (not shown).

⁴⁵Ca²⁺ Equilibrium Binding to GST-Fusion Proteins. The Ca²⁺ binding properties of the putative Ca²⁺ binding domain of the lobster RyR (LEF) and the corresponding regions of the rabbit skeletal (REF) and cardiac muscle (CEF) RyRs were determined by equilibrium dialysis using purified GST-fusion proteins. Nonspecific binding to the GST moiety of the fusion proteins was assessed using the purified GST protein under the same experimental conditions. Putative Ca²⁺ binding domain of lobster RyR specifically bound two Ca²⁺ at millimolar Ca²⁺ concentrations (Figure 3A). Hill plot analysis indicated that LEF specifically bound close to two Ca²⁺ with a Hill dissociation constant (*K_H*) of 0.9 mM

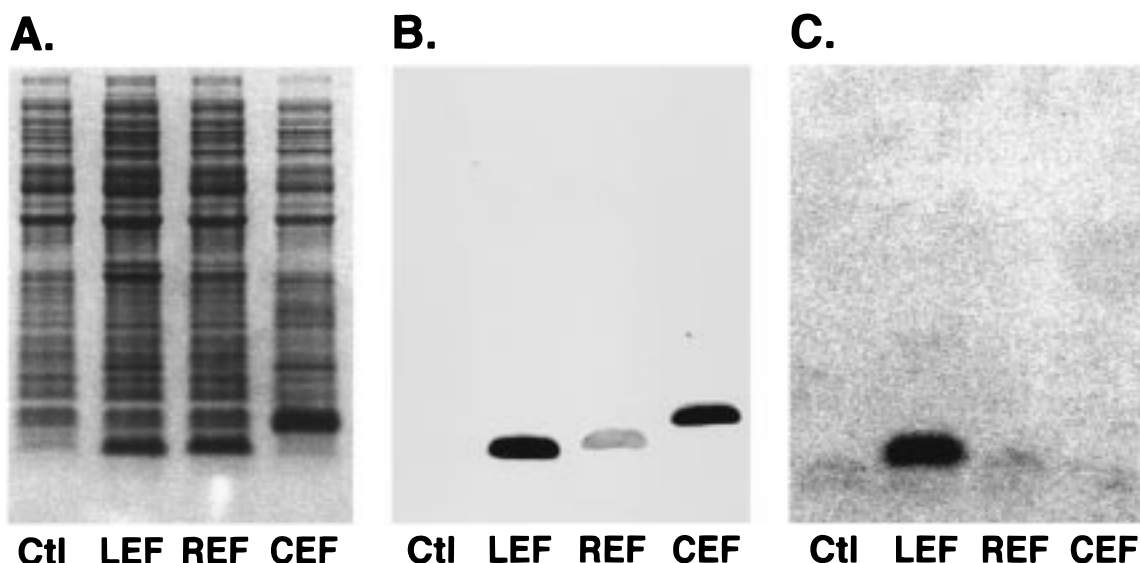


FIGURE 2: Analysis of fusion peptides LEF, REF, and CEF expressed in *E. coli*. Whole cell lysates (5–10 μ g) of *E. coli* strain BL21 containing pET vector (Ctl), LEF, REF, or CEF plasmids were denatured in SDS sample buffer and separated on 12% tricine–SDS–PAGE. (A) Gel stained with Coomassie Blue. (B) Immunoblot with T7•Tag monoclonal antibody. (C) Autoradiograph of a similar blot overlaid with a $^{45}\text{Ca}^{2+}$ -containing solution in 50 mM KCl, 10 mM imidazole, pH 6.8, and 3 μM $^{45}\text{Ca}^{2+}$ (2 $\mu\text{Ci/mL}$).

(Figure 3B). The Hill coefficient was 1.4, implying a weak positive cooperativity between the two EF-hand Ca^{2+} binding sites.

Figure 4A shows that $^{45}\text{Ca}^{2+}$ bound with a similar low affinity to REF and CEF. At the maximum free Ca^{2+} concentration used in this study (5 mM), REF and CEF bound about one Ca^{2+} . In constructing Hill plots, it was therefore necessary to consider two simple alternatives, namely that REF and CEF maximally bound one or two Ca^{2+} . Better fits were obtained assuming two Ca^{2+} binding sites ($R = 0.98$ vs 0.83, assuming one Ca^{2+} /REF or CEF). The Hill dissociation constant and coefficient for REF assuming two Ca^{2+} binding sites were 3.7 mM and 1.1, respectively (Figure 4B). The corresponding values for CEF were 3.8 mM and 1.3 (Figure 4B).

Ca^{2+} -Dependence of Lobster Skeletal Muscle RyR Activity. The Ca^{2+} activation/inactivation profile of the lobster Ca^{2+} release channel was determined in single-channel (Figures 5 and 6) and [^3H]ryanodine binding (Figure 7) measurements and compared with the $^{45}\text{Ca}^{2+}$ binding profile of LEF (Figure 8). Single channel measurements were performed by incorporating proteoliposomes containing the purified lobster channel (Figure 5) or SR vesicles (Figure 6) into planar lipid bilayers. Most of the single-channel measurements were carried out with purified channels, which simplified the measurements in two respects. First, K^+ and Cl^- SR channels that are also incorporated into the bilayer during SR vesicle fusion were absent. Second, channels could be incorporated and recorded in a monovalent cation medium. The lobster channel, similar to its mammalian counterparts, conducts monovalent cations more efficiently than Ca^{2+} and is essentially impermeable to Cl^- (17). In symmetric 250 mM KCl medium with K^+ as the current carrier, single-channel conductance was 775 pS (17). Single-channel activities were low at $\text{Ca}^{2+} < 1 \mu\text{M}$, reached a maximum value at $\sim 100 \mu\text{M}$ Ca^{2+} , and decreased again close to background levels as the Ca^{2+} concentration was increased to 10 mM (Figures 5A and 8).

In a previous study using passively loaded lobster SR vesicles, $^{45}\text{Ca}^{2+}$ efflux was optimally activated at 1–10 mM Ca^{2+} (17). Similarly, an optimal activation was observed at mM Ca^{2+} concentrations when purified CHAPS-solubilized lobster channel complexes were directly incorporated into the lipid bilayers. In contrast, in the present study purified channel complexes were freed of detergent by reconstitution into proteoliposomes before being incorporated into bilayers. It was therefore conceivable that the altered Ca^{2+} -sensitivity of the lobster channel observed in the previous lipid bilayer studies is an artifact resulting from the presence of detergent. In support of this suggestion, Figure 5B shows that the addition of 0.02% CHAPS returns the activity of a Ca^{2+} -inactivated channel (at 10 mM Ca^{2+}) to a level observed by Seok et al. (17).

To reconcile the different Ca^{2+} -dependence of the lobster RyR, we also performed single-channel measurements using lobster SR vesicles (Figure 6). Fusion of lobster SR vesicles was accomplished with the use of an asymmetric ion gradient (23). In preliminary experiments, we found that incorporation of lobster vesicles using K^+ - or Cl^- -containing media yielded a large number of channel activities. Unlike mammalian SR vesicles, lobster SR vesicles also contained channels that conducted Cs^+ with a high conductance (> 200 pS), which prevented the use of recording solutions containing Cs^+ . We selected an asymmetric 50 mM trans CaHepes, pH 7.3/0.8 M cis cholineCl, 0.5 mM CaCl_2 as the best condition for fusion of lobster SR vesicles with lipid bilayers as well as for obtaining Ca^{2+} -conducting channel activities. After perfusion of the cis (cytosolic) bilayer chamber with 125 mM Tris–250 mM Hepes, pH 7.3 solution containing 100 μM free Ca^{2+} , Cl^- conductances disappeared. A Ca^{2+} -conducting channel activity was observed in $< 10\%$ of the experiments after perfusion. Single-channel conductance was 99 pS, with Ca^{2+} as the current carrier (not shown). This conductance was essentially identical to that of native rabbit skeletal and canine cardiac muscle Ca^{2+} release channels recorded under the same ionic condition (23, 24). The native

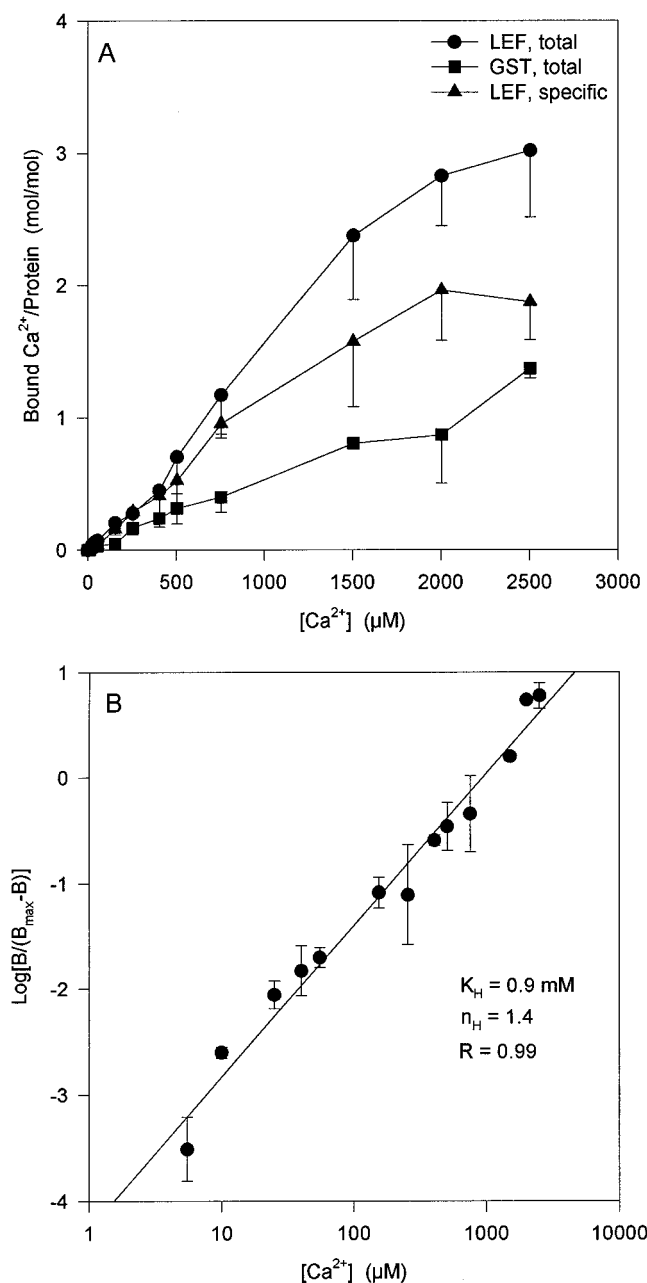


FIGURE 3: Equilibrium ⁴⁵Ca²⁺ binding to GST-LEF fusion protein. (A) Total ⁴⁵Ca²⁺ binding to purified GST-LEF (5–6 mg protein/mL) and GST (5–7 mg protein/mL) fusion proteins was determined by equilibrium binding dialysis as described in Experimental Procedures. Specific ⁴⁵Ca²⁺ binding to LEF represents the difference in ⁴⁵Ca²⁺ binding to LEF and GST fusion proteins. (B) Specific ⁴⁵Ca²⁺ binding data were plotted as a Hill plot assuming two Ca²⁺ binding sites per LEF. Values are the mean ±SE of 3–4 experiments.

Ca²⁺-conducting channels displayed a Ca²⁺-dependence comparable to that of purified channels. Single-channel activities were low at Ca²⁺ < 1 μM, reached a maximum value at ~1 mM Ca²⁺ ($P_o = 0.55 \pm 0.18$, $n = 3$), and decreased again close to background levels as the Ca²⁺ concentration was increased to 5 mM ($P_o = 0.12 \pm 0.12$, $n = 3$) (Figure 6).

Figure 7 shows the Ca²⁺-dependence of [³H]ryanodine binding to SR membranes from lobster skeletal, rabbit skeletal, and canine cardiac muscle. In each case, a biphasic Ca²⁺ activation/inactivation curve was obtained, with the

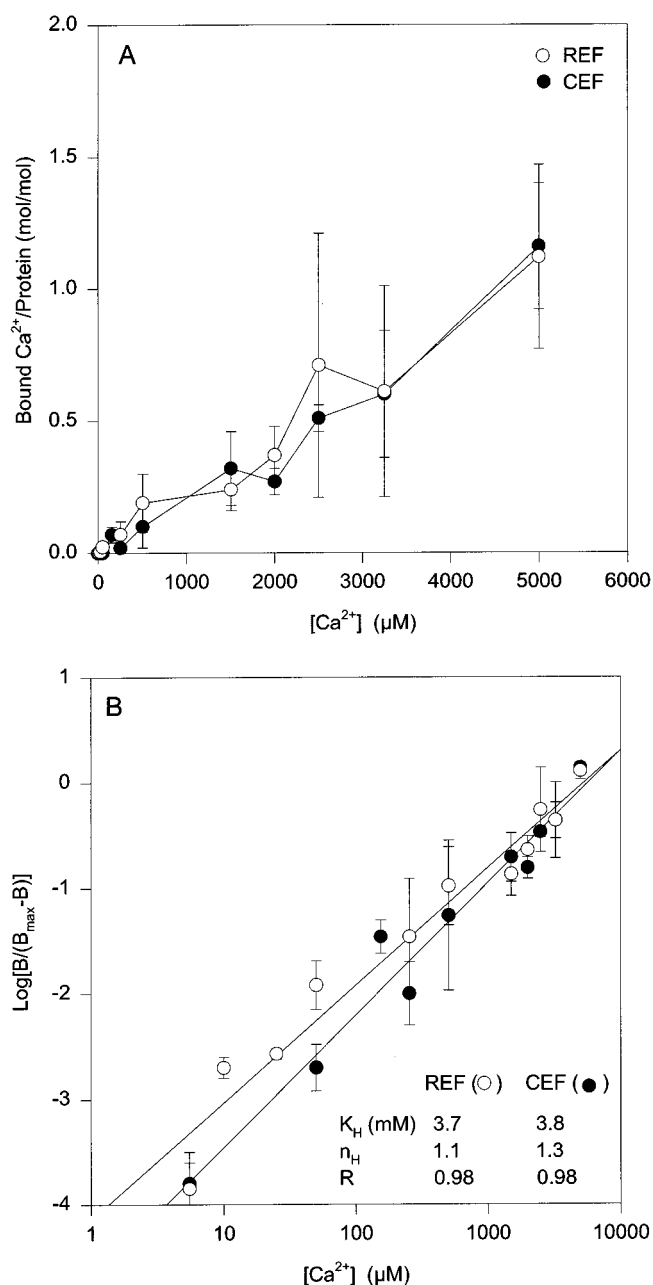


FIGURE 4: Equilibrium ⁴⁵Ca²⁺ binding to GST-REF and GST-CEF fusion proteins. (A) Specific ⁴⁵Ca²⁺ binding to REF (5–6 mg protein/mL) and CEF (4–6 mg protein/mL) was determined as in Figure 3. (B) Specific ⁴⁵Ca²⁺ binding data were plotted as Hill plots assuming two Ca²⁺ binding sites per REF and CEF. Values are the mean ±SE of 3–4 experiments. Where not indicated, error bars are equal to or smaller than symbols.

lobster RyR showing a Ca²⁺ dependence essentially identical to that of purified single-channel activities (Figures 5 and 8). The Ca²⁺-dependence of the lobster RyR differed from those of the mammalian counterparts in that higher Ca²⁺ concentrations were required for half-maximal activation of [³H]ryanodine binding. Ca²⁺ inactivation of lobster RyR matched that of the canine cardiac muscle RyR, with both requiring higher Ca²⁺ concentrations than the skeletal muscle RyR for half-maximal inhibition of [³H]ryanodine binding.

DISCUSSION

The present study made use of an affinity-purified anti-lobster RyR antibody to isolate four cDNA clones that

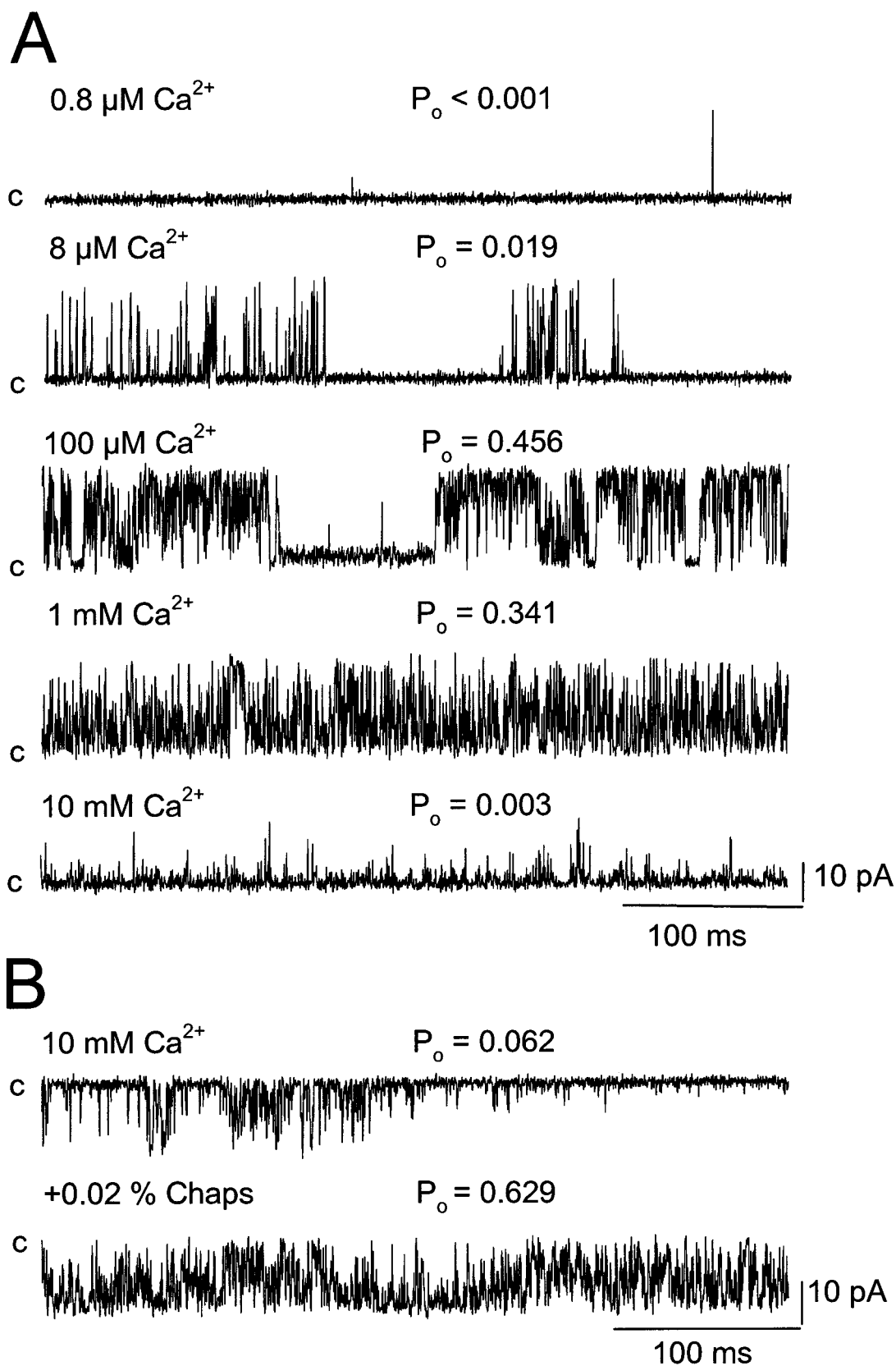


FIGURE 5: Ca^{2+} dependence of single purified lobster Ca^{2+} release channels in the absence and presence of detergent. Single-channel currents, shown as upward (A) and downward (B) deflections from closed levels (c on left), were recorded in symmetrical 250 mM KCl, 20 mM KPIPES, pH 7.0 media containing 0.1 mM EGTA and Ca^{2+} to yield the indicated free cytosolic Ca^{2+} concentrations. The trans chamber contained 8 μM free Ca^{2+} (0.1 mM EGTA and 0.1 mM Ca^{2+}). In (B) bottom trace, the cis chamber contained 0.02% CHAPS. An effect of added CHAPS on the Ca^{2+} activation/inactivation profile of the lobster RyR was observed in 3 out of 3 experiments. Holding potential was +35 mV (A) and -35 mV (B).

include 1513 carboxy-terminal amino acids of the lobster RyR. The deduced amino acid sequence encodes the

carboxy-terminal one-third of the lobster RyR and is homologous to other members of the RyR family. The

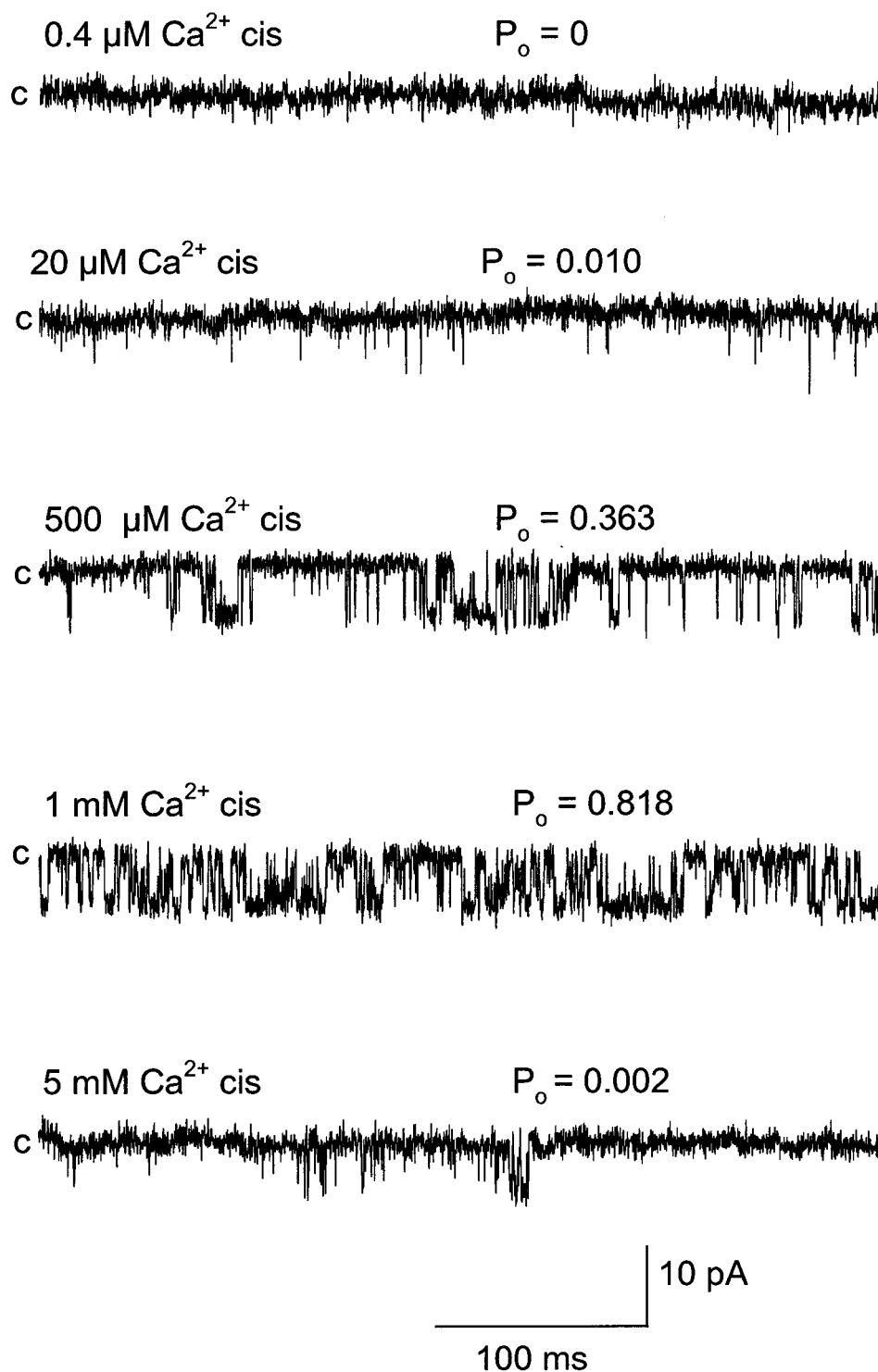


FIGURE 6: Ca²⁺-dependence of native lobster Ca²⁺ release channel. Single native lobster channel currents, shown as downward deflections from closed levels (c on left), were recorded in 50 mM trans CaHepes, pH 7.3/125 mM cis TrisHepes, pH 7.3 media containing 0.2 mM EGTA and Ca²⁺ to yield the indicated concentrations of free Ca²⁺. Holding potential was -35 mV. One of three similar single-channel recordings is shown.

carboxy-terminal portion of lobster RyR contains four putative channel-forming transmembrane stretches enriched in hydrophobic amino acids based on hydropathy analysis, as observed in the sequences of the other RyRs. Sequence analysis revealed a new two EF-hand Ca²⁺ binding domain (Figure 1A, bold letters) in the RyR family. ⁴⁵Ca²⁺ equilibrium binding studies suggest that this region may play an important role in the regulation of the lobster Ca²⁺ release channel as well as its mammalian counterparts.

Calcium ions are important, if not the principal, activators of all RyRs studied to date. For rabbit skeletal muscle RyR, in the absence of other regulatory ligands such as Mg²⁺ and ATP, a bell-shaped Ca²⁺ activation/inactivation curve is obtained in vesicle-Ca²⁺ efflux, single-channel, and [³H]-ryanodine measurements, with maximum activities at 10–100 μM Ca²⁺ (1, 2). Similarly, the mammalian cardiac RyR exhibits a biphasic response to Ca²⁺ with peak activation at 10–100 μM Ca²⁺, although inhibition by millimolar Ca²⁺

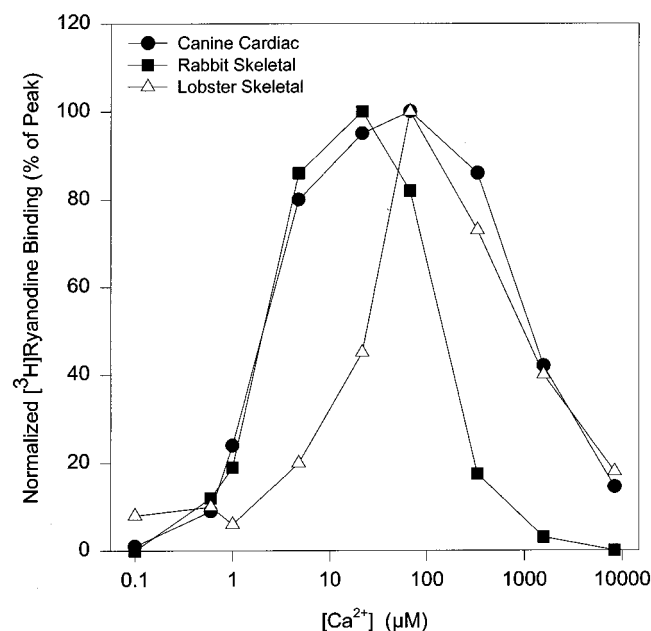


FIGURE 7: Ca^{2+} -dependence of $[^3\text{H}]$ ryanodine binding activities. $[^3\text{H}]$ Ryanodine binding to lobster skeletal muscle, rabbit skeletal muscle, and canine cardiac SR membranes was determined as described in Experimental Procedures. Peak values (100%) correspond to 0.14 ± 0.04 , 1.5 ± 0.3 , and 1.1 ± 0.2 pmol/mg protein for lobster skeletal muscle, rabbit skeletal muscle, and canine cardiac muscle membranes, respectively ($n = 3$).

is not as complete as that of skeletal RyR. These curves can be explained by the presence of high-affinity activating and low-affinity inactivating Ca^{2+} sites.

The Ca^{2+} activation/inactivation profile of lobster skeletal muscle RyR is less well-defined. In studies with passively (17, 25) and actively (unpublished studies) loaded SR vesicles from lobster (17, 25; unpublished studies) and crayfish (25) skeletal muscle, $^{45}\text{Ca}^{2+}$ efflux was optimally activated at 1–10 mM Ca^{2+} . Similarly, single lobster channels were optimally activated at mM Ca^{2+} concentrations (17). The previous single-channel measurements (17) were performed by directly incorporating the purified, CHAPS-solubilized, 30S channel complexes into the bilayers. Figure 5B suggests that the presence of detergent was responsible for the different Ca^{2+} dependence of single-channel activities observed in the present and previous study. Single-channel (26) and $[^3\text{H}]$ ryanodine binding (25, 27, 28) measurements using lobster SR vesicles yielded bell-shaped activation/inactivation curves, with peaks at $\sim 1 \mu\text{M}$ Ca^{2+} (26) or ranging from 10 to 100 μM Ca^{2+} (27, 28). A peak at $\sim 1 \mu\text{M}$ Ca^{2+} has been observed for the scallop RyR (K. E. Quinn and B. E. Ehrlich, personal communication).

As pointed out above, $^{45}\text{Ca}^{2+}$ flux measurements with passively loaded (17, 25) and actively loaded (17, 25, unpublished studies) lobster SR vesicles indicate a Ca^{2+} -dependence different from those observed in single-channel and $[^3\text{H}]$ ryanodine binding measurements. The differences appear to be unique to the lobster RyR because essentially the same Ca^{2+} dependence was observed for the mammalian RyRs in vesicle- $^{45}\text{Ca}^{2+}$ efflux, single-channel, and $[^3\text{H}]$ ryanodine binding measurements (not shown; see also refs 1, 2). One possible explanation for the different Ca^{2+} -dependence is that lobster SR vesicles contain a still to be identified ryanodine-insensitive Ca^{2+} conductance which is

activated at high Ca^{2+} concentrations but is of low conductance and therefore not readily detected in bilayer experiments.

To establish whether the EF-hand pair in lobster RyR and the corresponding regions of mammalian skeletal and cardiac muscle RyRs may play a role in Ca^{2+} regulation of the receptors, we expressed several fusion proteins corresponding to the sequence containing the EF-hand pair of lobster RyR. $^{45}\text{Ca}^{2+}$ overlays showed that LEF binds Ca^{2+} , but little, if any, binding was observed for REF and CEF following electrophoresis under denaturing conditions. $^{45}\text{Ca}^{2+}$ binding to REF and CEF might not have been detected in the overlays because of incomplete renaturation of Ca^{2+} binding sites. Two other possibilities we considered were a low binding affinity or the presence of kinetically labile binding sites. The EF-hand pair in lobster RyR and the corresponding regions of mammalian skeletal and cardiac muscle were therefore also expressed as soluble GST-fusion proteins, which allowed their isolation under nondenaturing conditions in quantities sufficient to determine their $^{45}\text{Ca}^{2+}$ binding properties by equilibrium binding analysis. These studies indicated that LEF maximally binds two Ca^{2+} . REF and CEF also appeared to bind two Ca^{2+} , although with a lower affinity than LEF. Because mammalian skeletal and cardiac RyRs are inhibited by Ca^{2+} at millimolar concentrations in both single-channel (2) and $[^3\text{H}]$ ryanodine (Figure 7) measurements, these data raise the possibility that the two EF-hand region initially identified in lobster RyR may play a role in Ca^{2+} -inactivation of mammalian RyRs. Similar Ca^{2+} binding affinity of REF and CEF is in apparent disagreement with observations that the cardiac RyR is less inhibited by mM Ca^{2+} than the skeletal muscle RyR (ref 2, see also Figure 7). Also, apparent Ca^{2+} binding affinity to LEF was about 4-fold higher than to REF, whereas $[^3\text{H}]$ ryanodine binding to lobster and skeletal RyRs suggested an opposite Ca^{2+} affinity. However, it is important to note that our $^{45}\text{Ca}^{2+}$ equilibrium binding experiments were done with small fragments of the RyRs and therefore might have detected Ca^{2+} binding pattern different from those in the native RyRs.

Interpretation of the binding data with regard to the role of LEF domain in lobster RyR is difficult due to differences in apparent Ca^{2+} dependence of RyR activation, as observed in SR vesicle- Ca^{2+} flux, single-channel, and $[^3\text{H}]$ ryanodine binding measurements (see above). Since lobster and mammalian RyRs can be isolated as 30S channel complexes and the identity of amino acid sequences among RyR isoforms is very high (70%), it is likely that different RyR isoforms have a similar overall structure. REF and CEF have Ca^{2+} affinities that suggest they may be Ca^{2+} inhibition sites. Based on the high similarity of peptide sequence among LEF, REF, and CEF, LEF may then also be a Ca^{2+} inactivation site. The most direct evidence supporting a Ca^{2+} inactivation site in lobster RyR is provided by single-channel measurements (Figures 5, 6, and 8).

Analysis of the primary sequence of mammalian RyRs shows that there are regions of RyR1 (3), RyR2 (5), and RyR3 (7) that bear some resemblance to the EF-hand Ca^{2+} binding motif. None of these regions overlaps with the region of lobster RyR containing the predicted EF-hand structures, except that RyR3 has an EF-handlike sequence which corresponds to the first EF-hand sequence of lobster RyR. To our knowledge, the Ca^{2+} binding properties of the

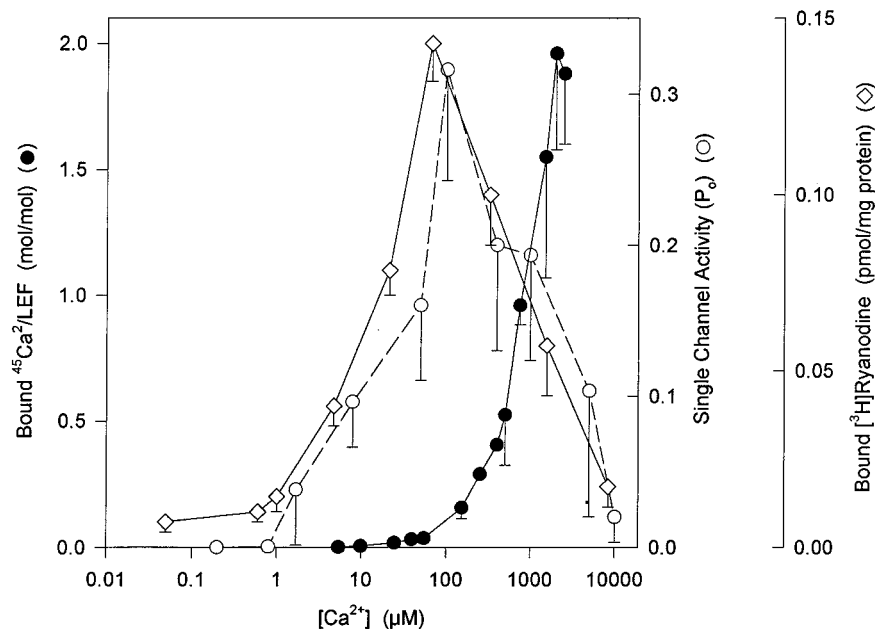


FIGURE 8: $^{45}\text{Ca}^{2+}$ equilibrium binding to LEF and Ca^{2+} activation/inactivation profiles of lobster skeletal muscle RyR. Specific $^{45}\text{Ca}^{2+}$ binding to GST-LEF was determined as described in Figure 3 ($n = 3-4$). Ca^{2+} -dependence of single purified channel activities ($n = 3-18$) and $[^3\text{H}]\text{ryanodine}$ binding ($n = 3$) were determined as described in Figures 5A and 7, respectively. Values are the mean \pm SE.

predicted EF-handlike structures of RyR2 and RyR3 have not been reported.

Ca^{2+} binding properties of rabbit skeletal muscle RyR were studied using $^{45}\text{Ca}^{2+}$ and ruthenium red overlays of bacterial fusion proteins containing RyR1 fragments (29, 30). Five potential Ca^{2+} binding domains were identified: an N- and C-terminal region, two acidic regions in the middle of RyR, and a region containing the three EF-handlike structures predicted by Takeshima et al. (3). Ca^{2+} binding to the last region was further mapped to three subregions, each encompassing one EF-handlike structure. An antibody directed against one of the subregions increased the Ca^{2+} sensitivity of skeletal muscle Ca^{2+} release channels incorporated into planar lipid bilayers, whereas an antibody against another subregion was inhibitory (30). A fusion peptide containing the REF region was a minor Ca^{2+} binding protein among the fusion proteins expressed by Chen et al. (29), but was not further characterized by those investigators.

There are two kinds of EF-hand sites that are classified according to their ion selectivity: Ca^{2+} -specific sites and $\text{Ca}^{2+}/\text{Mg}^{2+}$ mixed sites. The Ca^{2+} -specific sites bind only Ca^{2+} , whereas the $\text{Ca}^{2+}/\text{Mg}^{2+}$ mixed sites bind both ions and bind Ca^{2+} with a very high affinity (10^{-7} – 10^{-9} M) (13). The $\text{Ca}^{2+}/\text{Mg}^{2+}$ site of smooth muscle myosin regulatory light chain was converted into a Ca^{2+} -specific site by replacing an aspartic acid in position -Z of Ca^{2+} binding loop of EF-hand (Figure 1B) with a glutamic acid (31). Both EF-hand motifs of LEF have an aspartic acid residue in position of -Z, suggesting LEF may be a $\text{Ca}^{2+}/\text{Mg}^{2+}$ mixed site. However, an argument against this suggestion is that the Ca^{2+} binding affinity of LEF ($\sim 10^{-3}$ M) is more than a thousand times lower than that of the typical $\text{Ca}^{2+}/\text{Mg}^{2+}$ mixed sites (10^{-7} – 10^{-9} M). Despite extensive investigation (32–36), the origin of specificity and affinity of Ca^{2+} binding domains is not clear. One reason is that conformational changes in the loop region of an EF-hand appear to be necessary to obtain a high ion binding selectivity. Therefore,

it is difficult, if not impossible, to predict the ion selectivity of EF-hand from its primary structure (31).

While fusion proteins containing RyR fragments are useful tools to probe for structures responsible for RyR regulation, mutagenesis would provide a more direct picture of the structure–function relationship. The biochemical and electrophysiological properties of the lobster skeletal muscle RyR and its mammalian counterparts have been characterized extensively. Differences in their responses to Ca^{2+} (Figure 7) and the Ca^{2+} binding properties of LEF and corresponding mammalian sequences (Figures 2–4) make them favorable pairs to construct chimeras for obtaining information on the structure–function relationship and regulatory mechanisms of this unique family of ion channels.

REFERENCES

1. Coronado, R., Morrisette, J., Sukhareva, M., and Vaughan, D. M. (1994) *Am. J. Physiol.* 266, C1485–C1504.
2. Meissner, G. (1994) *Annu. Rev. Physiol.* 56, 485–508.
3. Takeshima, H., Nishimura, S., Matsumoto, T., Ishida, H., Kangawa, K., Minamino, N., Matsuo, H., Ueda, M., Hanaoka, M., Hirose, T., and Numa, S. (1989) *Nature* 339, 439–445.
4. Zorzato, F., Fujii, J., Otsu, K., Phillips, M., Green, N. M., Lai, F. A., Meissner, G., and MacLennan, D. H. (1990) *J. Biol. Chem.* 265, 2244–2256.
5. Nakai, J., Imagawa, T., Hakamata, Y., Shigekawa, M., Takeshima, H., and Numa, S. (1990) *FEBS Lett.* 271, 169–177.
6. Otsu, K., Willard, H. F., Khanna, V. K., Zorzato, F., Green, N. M., and MacLennan, D. H. (1990) *J. Biol. Chem.* 265, 13472–13483.
7. Hakamata, Y., Nakai, J., Takeshima, H., and Imoto, K. (1992) *FEBS Lett.* 312, 229–235.
8. Oyama, H., Murayama, T., Takagi, T., Iino, M., Iwabe, N., Miyata, T., Ogawa, Y., and Endo, M. (1994) *J. Biol. Chem.* 269, 17206–17214.
9. Ottini, L., Marziali, G., Conti, A., Charlesworth, A., and Sorrentino, V. (1996) *Biochem. J.* 315, 207–216.
10. Takeshima, H., Nishi, M., Iwabe, N., Miyata, T., Hosoya, T., Masai, I., and Hotta, Y. (1994) *FEBS Lett.* 337, 81–87.

11. Phillips, M. S., Fujii, J., Khanna, V. K., DeLeon, S., Yokobata, K., de Jong, P. J., and MacLennan, D. H. (1996) *Genomics* 34, 24–41.
12. Kretsinger, R. H., and Nockolds, C. E. (1973) *J. Biol. Chem.* 248, 3313–3326.
13. Celio, M. R., Pauls, T., and Schwaller, B. (1996) *Guidebook to the Calcium-Binding Proteins*, Sambrook and Tooze Publication at Oxford University Press, New York.
14. Atwood, H. L. (1972) in *The Structure and Function of Muscle* (Bourne, G. H., Ed.) Vol. 1, pp 421–489, Academic Press, New York.
15. Gyorke, S., and Palade, P. (1992) *J. Physiol.* 457, 195–210.
16. Chomczynski, P., and Sacchi, N. (1978) *Anal. Biochem.* 162, 156–159.
17. Seok, J. H., Xu, L., Kramarcy, N. R., Sealock, R., and Meissner, G. (1992) *J. Biol. Chem.* 267, 15893–1590.
18. Maruyama, K., Mikawa, T., and Ebashi, S. (1984) *J. Biochem.* 95, 511–519.
19. Schagger, H., and von Jagow, G. (1987) *Anal. Biochem.* 166, 368–379.
20. Lee, H. B., Xu, L., and Meissner, G. (1994) *J. Biol. Chem.* 269, 13305–13312.
21. Tripathy, A., Xu, L., Mann, G., and Meissner, G. (1995) *Biophys. J.* 69, 106–119.
22. Schoenmakers, J. M., Visser, G. J., Flick, G., and Theuvene, A. P. R. (1992) *BioTechniques* 12, 870–879.
23. Smith, J. S., Coronado, R., and Meissner, G. (1986) *J. Gen. Physiol.* 88, 573–588.
24. Rousseau, E., Smith, J. S., Henderson, J. S., and Meissner, G. (1986) *Biophys. J.* 50, 1009–1014.
25. Seok, J. H., Jung, J. K., Hur, G. M., and Lee, J. H. (1994) *Korean J. Pharm.* 30, 125–136.
26. Quinn, K. E., and Ehrlich, B. E. (1997) *Biophys. J.* 72, A358.
27. Formelova, J., Hurnak, O., Novotova, M., and Zachar, J. (1990) *Gen. Physiol. Biophys.* 9, 445–453.
28. Olivares, E., Arispe, N., and Rojas, E. (1993) *Membr. Biochem.* 10, 221–235.
29. Chen, S. R. W., Zhang, L., and MacLennan, D. H. (1992) *J. Biol. Chem.* 267, 23318–23326.
30. Chen, S. R. W., Zhang, L., and MacLennan, D. H. (1993) *J. Biol. Chem.* 268, 13414–13421.
31. da Silva, A. C. R., Kendrick-Jones, J., and Reinach, F. C. (1995) *J. Biol. Chem.* 270, 6773–6778.
32. Reid, R. E., Gariepy, J., Saund, A. K., and Hodges, R. S. (1981) *J. Biol. Chem.* 256, 2742–2751.
33. Hapak, R. C., Lammers, P. J., Palmisano, W. A., Birnbaum, E. R., and Henzl, M. T. (1989) *J. Biol. Chem.* 264, 18751–18760.
34. Marsden, B. J., Shaw, G. S., and Sykes, B. D. (1990) *Biochem. Cell Biol.* 68, 587–601.
35. Pauls, T. L., Durussel, I., Cox, J. A., Clark, I. D., Szabo, A. G., Gagne, S. M., Sykes, B. D., and Berchtold, M. W. (1993) *J. Biol. Chem.* 268, 20897–20903.
36. Procyshyn, R. M., and Reid, R. E. (1994) *J. Biol. Chem.* 269, 1641–1647.

BI971198B